Springer

KSME

Journal of Mechanical Science and Technology 24 (11) (2010) 2189~2195
www.springerlink.com/content/1738-494x
DOI 10.1007/s12206-010-0905-3

Numerical analysis method to estimate thermal deformation of a ventilated disc for automotives †

Won Sun Chung[1], Sung Pil Jung[2] and Tae Won Park[3,*]

[1]*Body Chassis Reliability Team, Korea Automotive Technology Institute, Chonan, 330-912, Korea*
[2]*Graduate School of Mechanical Engineering, Ajou University, Suwon, 443-749, Korea*
[3]*Department of Mechanical Engineering, Ajou University, Suwon, 443-749, Korea*

(Manuscript Received June 16, 2010; Revised July 12, 2010; Accepted August 24, 2010)

Abstract

This paper presents an analysis method to estimate the thermal performance of a disc in a vehicle considering braking conditions and the characteristics of hydraulic devices such as the booster, master cylinder and proportional valve. The whole braking pressure transfer process in the hydraulic brake system from its generating by the pedal to action on the pad is analytically determined. The heat flux generated in the disc brake module is calculated by assuming that the braking energy changes into thermal energy. Heat flux is applied to the finite element disc model, and the temperature rise and deformation of a disc are estimated by performing the thermo-mechanical analysis. The analysis results are discussed and the analytical process and simulation model are verified.

Keywords: Thermal performance; Hydraulic devices; Heat flux; Disc brake; Finite element analysis model; Thermo-mechanical analysis

1. Introduction

The ventilated discs used in the brake system of automobiles require rapid cooling performance and robust structural design to prevent thermal deformation since their temperature increases greatly during braking. The braking performance of a vehicle is significantly affected by the temperature rise of the brake system. A disc with good cooling performance can control its temperature rise and prevent thermal-related problems such as hot judder, which is caused by the thermal deformation of the disc, rapid wearing of the pad and vapor lock of the brake oil caused by the heat transfer to the caliper. Therefore, in the early design stage, the temperature increase and thermal performance of a disc need to be predictable.

Thermal characteristics of a disc have been estimated and analyzed in many studies. Faramarz [1] extracted the governing equations for heat transfer on a simple disc and pad assembly and solved the equations using Green's function approach. Faramarz calculated the temperature rise of the disc by assuming that all of the kinetic energy of a vehicle was converted into thermal energy. Kim [2] investigated the effects of design parameters for a ventilated disc on the temperature distribution of the disc surface by using a three-dimensional unsteady model created by FLUENT. Choi [3] compared the thermal dissipation performance of two discs: one had normal vents and the other had helical grooved vents. Choi used a finite element analysis technique and simulated a piece of the disc under the repeated braking mode. Kim [4] proposed the analysis method using FE software (ANSYS) to predict the temperature distribution and thermal deformation of a disc. Hwang [5] conducted a thermo-mechanical coupling analysis of a partial three-dimensional disc brake model and discussed the temperature and contact pressure distributions of a disc. These studies are not sufficient for predicting the temperature rise of a disc as vehicle and brake information and the mechanical characteristics of the hydraulic components of the brake system are not considered. Most studies assumed that one-fourth of the kinetic energy of a vehicle was fully changed into thermal energy under ideal braking circumstances and calculated the heat flux to be applied to the disc brake module. Thus, the change in the mechanical energy of a vehicle according to the performance of its hydraulic brake system and braking condition could not be considered in the simulation model.

In this study, the transfer process of the braking pressure in a hydraulic brake system is determined mathematically [6], and the heat flux, which is applied to the disc, is calculated. Braking energy is assumed to convert into thermal energy, and the heat flux division between the disc and pad is computed using a one-dimensional heat conduction model [7]. A three- dimen-

† This paper was recommended for publication in revised form by Associate Editor Yeon June Kang

*Corresponding author. Tel.: +82312192952, Fax: +82312191965
E-mail address: park@ajou.ac.kr

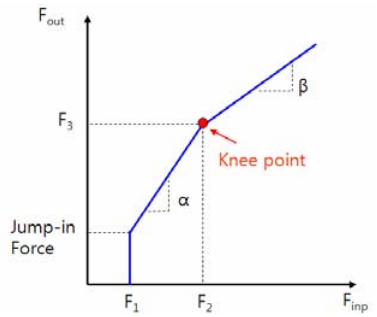

Fig. 1. Booster characteristic curve.

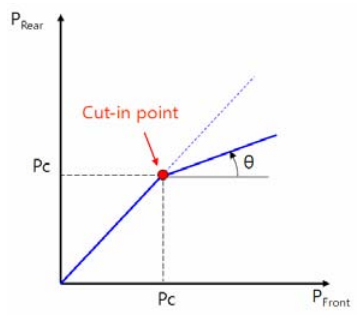

Fig. 2. P-valve characteristic curve.

sional finite element model is created using SAMCEF [8], and the thermo-mechanical analysis is performed to estimate the temperature rise and thermal deformation of a disc.

2. Analytical process to calculate heat flux to a disc in a hydraulic brake system

2.1 Analytical braking process

Braking of a vehicle starts when a driver steps on the brake pedal. The pedal effort, which is the force applied to the brake pedal by the driver, is increased through a booster. A vacuum booster is generally used, and its mechanical characteristic is shown in Fig. 1. In Fig. 1, F_{inp} and F_{out} are the input and output forces of the booster, and 'Jump-in Force' is the output force of the booster when the input force is greater than the threshold load (F_1). α and β are the first and second boosting ratios. The boosting ratio is changed at 'Knee point' where the input and output forces of the booster are F_2 and F_3, respectively. The input force of the booster is calculated as

$$F_{inp} = (F_P - F_0)\gamma_p \eta_p \,, \tag{1}$$

where F_P is the pedal effort, F_0 is the pedal loss force, γ_p is the pedal ratio and η_p is the pedal efficiency. The output force of the booster is calculated as

$$F_{out} = \begin{cases} 0 & (F_{inp} < F_1) \\ \alpha(F_{inp} - F_1) + Jump & (F_1 \le F_{inp} < F_2) \\ \beta(F_{inp} - F_2) + F_3 & (F_{inp} \ge F_2) \end{cases} . \tag{2}$$

The output force of the booster changes into the hydraulic pressure (LP_M) through the master cylinder as

$$LP_M = (F_{out} - F_{loss}) / A_{M.cylinder} \,, \tag{3}$$

where F_{loss} is the master cylinder resist force, and $A_{M.cylinder}$ is the cross sectional area of the master cylinder piston.

The braking pressure transferred to the front axle should be greater than that transferred to the rear axle since the front axle weight increases during braking. A valve is used to control the amounts of front and rear braking pressures. Fig. 2 shows the characteristic of the proportional valve.

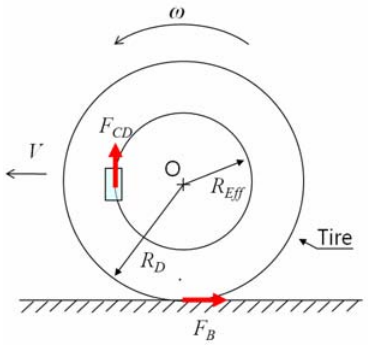

Fig. 3. Braking configuration of disc brakes.

Fig. 2 shows the braking pressures applied to the front and rear brake modules, P_{Rear} and P_{Front}. The magnitude of P_{Rear} is the same as that of P_{Front} before the 'Cut-in point', and after 'Cut-in point', and P_{Front} increases at a constant slope of θ. The pressure at 'Cut-in point' is called the critical pressure P_C. The hydraulic braking pressures transferred to the front and rear brake modules (P_{Front} and P_{Rear}) are computed as

(1) Before 'Cut-in point'

$$P_{Front} = P_{Rear} = \frac{LP_M}{2} \,. \tag{4}$$

(2) After 'Cut-in point'

$$\begin{cases} P_{Front} = \dfrac{LP_M - (1 - \tan\theta)P_C}{(1 + \tan\theta)} \\ P_{Rear} = LP_M - P_{Front} \end{cases} \tag{5}$$

The threshold pressure, which is the pressure lost until the braking begins, is ignored in Eqs. (4) and (5) since its amount is relatively small.

When a vehicle is under braking, the caliper drag (F_{CD}), which is the friction force between the disc and pad, is generated as shown in Fig. 3. In Fig. 3, V is the vehicle speed, ω is the rotational speed of a wheel, R_{Eff} and R_D are the effective and dynamic radii of a tire.

The caliper drag of the disc brake is calculated as

$$F_{CD} = \mu P_B A_C \eta_C \,, \tag{6}$$

where μ is the friction coefficient between the disc and pad, P_B is the braking pressure, A_C is the cross sectional area of the caliper piston and η_C is the caliper efficiency. During braking, the total actual braking force (F_B) can be obtained through the moment equilibrium equation at the center (O) of a tire.

$$F_B = \{(F_{CD}R_{Eff})_{Front} + (F_{CD}R_{Eff})_{Rear}\} / R_D \,, \tag{7}$$

where the subscripts $_{Front}$ and $_{Rear}$ mean the front and rear axle brakes. The total braking force should be the same as the inertial force of the vehicle as

$$F_B = W \cdot a \,, \tag{8}$$

where W is the total weight of the vehicle and a is the deceleration whose unit is g. Therefore, the deceleration of a vehicle can be written as

$$a = F_B / W \,. \tag{9}$$

2.2 Calculation of the heat flux to a disc

The front axle braking torque ($T_{Axle,front}$) is represented as

$$T_{Axle.front} = (R_{Eff} F_{CD})_{Front} \,. \tag{10}$$

The front axle braking power ($P_{Axle,front}$) can be obtained by multiplying the braking torque by the rotational speed of the wheel as

$$P_{Axle.front} = \omega T_{Axle.front} \,. \tag{11}$$

Considering the slip ratio λ, Eq. (5) can be changed as

$$P_{Axle.front} = \frac{V(1-\lambda)}{R_D} T_{Axle.front} \,. \tag{12}$$

The front tire friction power ($P_{Tire,front}$), which is generated by the slip of the tire, can be calculated by using the friction force between the tire and road as

$$P_{Tire.front} = \mu_g W_F \lambda V \,, \tag{13}$$

where μ_g is the friction coefficient between the tire and road and W_F is the front axle weight. W_F can be obtained according to the dynamic axle weight distribution of a vehicle as shown in Fig. 4.

In Fig. 4, W is the total weight of the vehicle, h is the C.G height, L is the length of the wheel base, L_F and L_R are the distances from the contact points of the front and rear tires and road surface to the C.G point. a is the deceleration, W_F and W_R are the dynamic front and rear weights, and B_F and B_R are the front and rear braking forces, respectively. The moment equations at contact points between the front and rear tires and road surface are as follows:

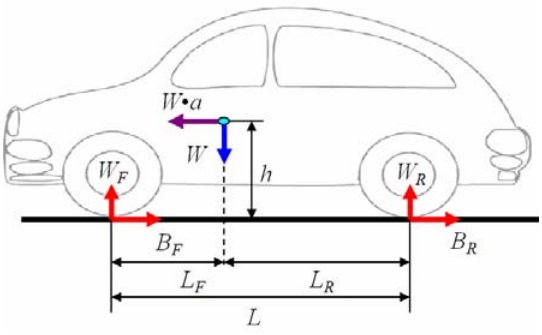

Fig. 4. Dynamic axle weight distribution of a vehicle.

$$\begin{cases} \sum M_F = W_R L + Wah - WL_F = 0 \\ \sum M_R = -W_F L + Wah + WL_R = 0 \end{cases}. \tag{14}$$

Thus, W_F and W_R can be written as

$$\begin{cases} W_F = (L_R + ha)W / L \\ W_R = (L_F - ha)W / L \end{cases}. \tag{15}$$

The front braking power, which is generated at the front axle of a vehicle, is the sum of the front axle braking power and front tire friction power. Assuming that the total kinetic energy of a vehicle is completely changed to thermal energy without any loss, the braking power supplies heat to a disc as heat flux as follows:

$$\begin{aligned} P_{Braking.front} &= P_{Axle.front} + P_{Tire.front} \\ &= \frac{V(1-\lambda)}{R_D} T_{Axle.fornt} + \mu_g W_F \lambda V \\ &= Aq'' \end{aligned} \tag{16}$$

where A is the contact area between the disc and pad.

2.3 Heat flux division into the disc and pad

The heat flux generated from the braking power is divided between the disc and pad. Fig. 5 shows a one-dimensional heat conduction model of a disc and pad. If the friction heat is transferred to the disc and pad without any loss, the heat fluxes applied to the surface of the disc and pad are q_d'' and q_p'', respectively. Using the heat transfer equation for a semi-infinite solid, the relation between the temperature (T_j) and heat flux (q_j'') of body j is given as

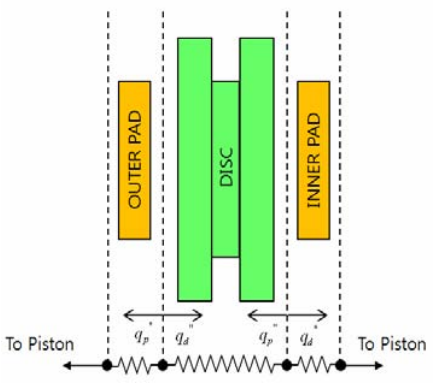

Fig. 5. One dimensional heat conduction model of the disc brake module.

$$T_j(x,t) = \frac{2q_j^{"}\sqrt{k_j \cdot t}}{v_j} \cdot ierfc(\frac{x}{2\sqrt{k_j \cdot t}}), \quad (17)$$

where x is the length to the end face of body j, t is the time of heat transfer, v_j and k_j are the thermal diffusivity and thermal conductivity of body j, respectively. *ierfc*, which is the first repeated complementary error function, is calculated as

$$ierfc(x) = \int_x^\infty erfc(x)dx = \frac{1}{\sqrt{\pi}}e^{-x^2} - xerfc(x), \quad (18)$$

where the complementary error function *erfc* is defined as

$$erfc(x) = \frac{2}{\sqrt{\pi}}\int_x^\infty e^{-\zeta^2}d\zeta. \quad (19)$$

Because the temperatures on the friction surface between the disc and pad should be the same, Eq. (20) acts as the boundary condition.

$$T_d(0,t) = T_p(0,t), \quad (20)$$

where T_d and T_p are the temperatures of the disc and pad. By applying Eq. (20) to Eq. (17), the ratio (ξ) of the heat flux transferred to the disc of the total heat flux can be calculated as

$$\xi = \frac{q_d^{"}}{q_d^{"} + q_p^{"}} = \frac{1}{1 + \sqrt{\frac{k_p}{k_d} \cdot \frac{\rho_d c_d}{\rho_p c_p}}}, \quad (21)$$

where ρ_d and ρ_p are the mass densities of the disc and pad, and c_d and c_p are the specific heats of the disc and pad, respectively. Therefore, the heat flux per unit area applied to one side of the front disc (q_d'') is given by the following equation:

Table 1. Vehicle and brake information.

Vehicle information		
Vehicle weight (kgf)	2230.0	
Front axle weight (kgf)	1280.0	
C.G height (mm)	669.0	
Length of wheelbase (mm)	2710.0	
Slip ratio (%)	95.0	
Dynamic radius of tire (mm)	361.0	
Pedal ratio	4.1	
Brake information		
Category	Front	Rear
Diameter of wheel cylinder (mm)	46.0	43.0
Caliper efficiency (%)	100.0	100.0
Brake effective radius (mm)	126.0	134.0
Specific heat of disc (J/kg°C)	642	
Specific heat of pad (J/kg°C)	1465	
Thermal conductivity of disc (W/m°C)	53	
Thermal conductivity of pad (W/m°C)	1.5	
Mass density of disc (kg/m^3)	7200	
Mass density of pad (kg/m^3)	2150	
Hydraulic device information		
Booster Jump-in force (kgf)	50	
Booster first input force (kgf)	6.46	
Booster second input force (kgf)	57.1	
First boosting ratio	9	
Second boosting ratio	1	
Diameter of master cylinder (mm)	27	
Critical pressure of P-valve (bar)	35	
Reduce slope of P-valve	0.25	

$$q_d^{"} = \frac{1}{4}\xi q^{"}. \quad (22)$$

3. Braking conditions and heat flux generation

The heat flux for the front disc was calculated by using Eq. (22) for a vehicle whose initial speed was 130 km/h was braking for 5 seconds. The friction coefficients of road and pad were set as 0.7 and 0.8, respectively, and the information about the vehicle, brake and hydraulic device is shown in Table 1.

Fig. 6(a)-(d) show the braking conditions and calculated heat flux per unit area of a disc. Fig. 6(a) shows the pedal effort profile which is the source force for braking. The pedal effort increases linearly until t = 0.5 s, and remains at a constant level of 15 kgf. Fig. 6(b) shows the booster input and output forces. The booster output force is zero until the booster input force reaches 6.46 kgf, and then increases sharply from the jump-in force of 50 kgf.

Fig. 6(c) represents the braking pressure distribution. The magnitudes of the front and rear braking pressures differ from

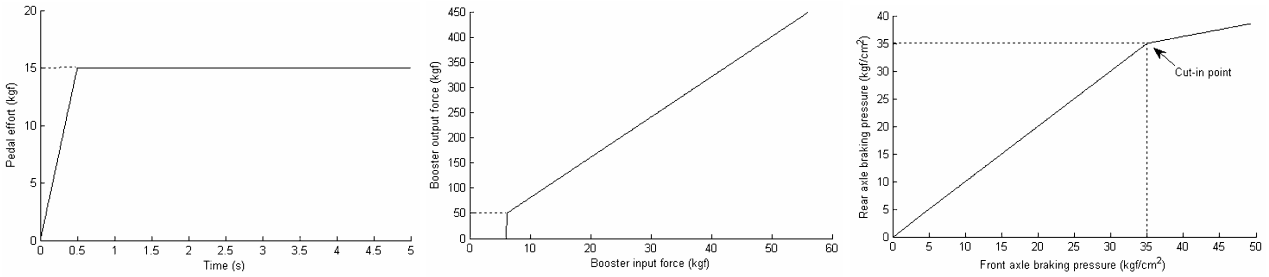

(a) Pedal effort profile (b) Booster input / output force curve (c) Braking pressure distribution

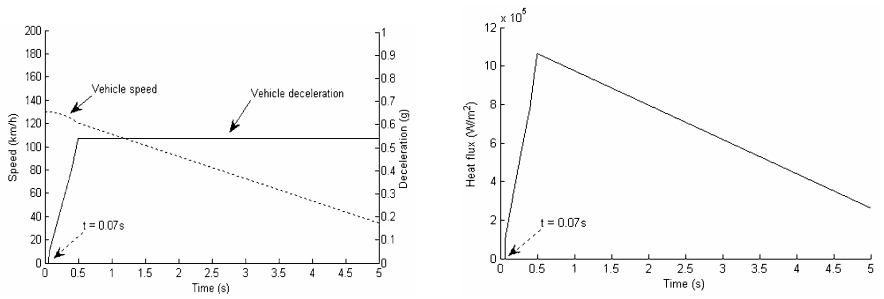

(d) Variation of the vehicle speed and deceleration (e) Heat flux applied per unit area of a disc

Fig. 6. Braking condition and heat flux profiles.

the cut-in point with a constant slope of 0.25, and the front and rear pressures are 35 kgf/cm^2 at this point. Fig. 6(d) shows how the vehicle speed and deceleration change. The vehicle begins to decelerate at t = 0.07 s, and its speed decreases from 130 km/h to 34.4 km/h. The deceleration of a vehicle reaches its highest value of 0.54 g at t = 0.5 s, and remains constant. Using the results of Figs. 6(a)-(d), the heat flux is obtained as shown in Fig. 6(e). The heat flux is generated from t = 0.07 s, and has the maximum value of 1.12 MW/m^2 at t = 0.5 s.

4. Thermo-mechanical analysis of a disc

To predict the temperature rise and thermal deformation of a disc when the heat flux shown in Fig. 6(e) is applied to the disc, a thermo-mechanical analysis was done using the commercial finite element analysis program, SAMCEF. First, the transient heat transfer analysis was performed using SAMCEF/Thermal, and the temperature rise of a disc according to time was saved. The temperature rise history of the thermal model was applied to the mechanical model as thermal load, and the thermal deformation of the mechanical model was calculated. This nonlinear structural analysis was carried out using SAMCEF/Mechano.

4.1 Finite element model of a disc

Fig. 7 shows the finite element model of a disc and the boundary conditions. The finite element model is created using a 4-node tetrahedron element and has 4,363 nodes and 18,368 elements. Heat flux shown in Fig. 6(e) is applied to both contact areas of the disc and two pads. The initial temperature of the disc is 80℃, and the surface convection condition with the reference temperature of 25℃ and the convection coefficient of 40 W/m^2℃ is applied to the all contact areas of the disc and air. Thermal properties of the disc material are shown in Table 1. For the mechanical properties, the elastic modulus of 135 GPa, Poisson's ratio of 0.29 and the thermal expansion coefficient of 1.05e-5 /℃ are used.

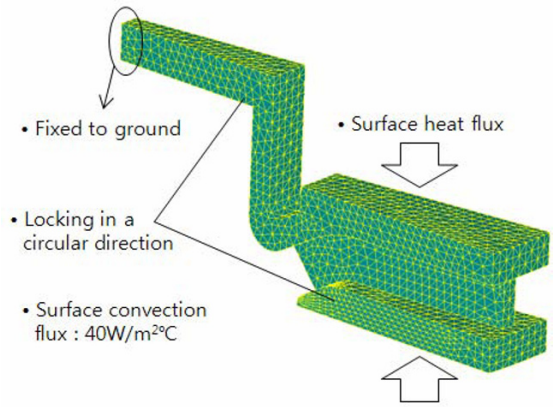

Fig. 7. Finite element model and boundary conditions for thermo-mechanical analysis of a disc.

4.2 Thermo-mechanical analysis results

Figs. 8(a) and (b) show the thermal analysis results. In Fig. 8(a), the nodal temperature distribution of the disc at t = 5 s is described. Temperature is concentrated at the central region of the rotational axis of the inner board of the disc. Fig. 8(b) shows the temperature rise of the disc, which is measured at the point shown in Fig. 8(a). The disc temperature remains

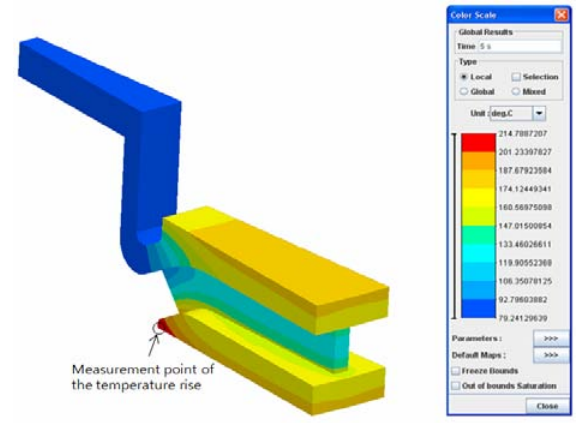

(a) Nodal temperature distribution of a disc

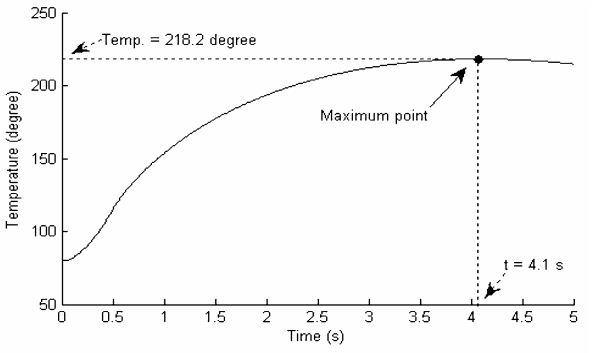

(b) Temperature rise of a disc

Fig. 8. Thermal analysis results.

80 °C until t = 0.7 s, and then increases and reaches its maximum value of 164.4 °C at t = 4.1 s. The disc temperature decreases after t = 4.1 s since the heat loss by convection heat transfer to the air is greater than the heat generation by heat flux. The nodal temperature distribution history was saved, and applied to the mechanical model as a temperature load.

Figs. 9(a) and (b) show the mechanical analysis results. Fig. 9(a) shows the nodal displacement distribution of the disc at t = 5 s. The deformation of the disc material gradually increases in the radial direction of the disc, and becomes the highest at the circumference region. Fig. 9(b) shows the disc thickness variation (DTV). The disc thickness is defined Fig. 9(a). In Fig. 9(b), the initial disc thickness expansion is 102.6 μm, and the disc thickness expansion is reduced until t = 1.2 s. This is because the potential energy due to the thermal expansion of the material by the initial temperature of 80 °C is larger than the thermal energy transferred to the disc for a certain amount of time as shown in Fig. 9(c). The amount of the potential energy is almost the same as the amount of thermal energy around t = 3 s, and then the disc thickness expands to more than its initial value. The maximum DTV, which is defined as the difference between the initial and final values of the disc thickness as shown in Fig. 9(b), is 13.2 μm.

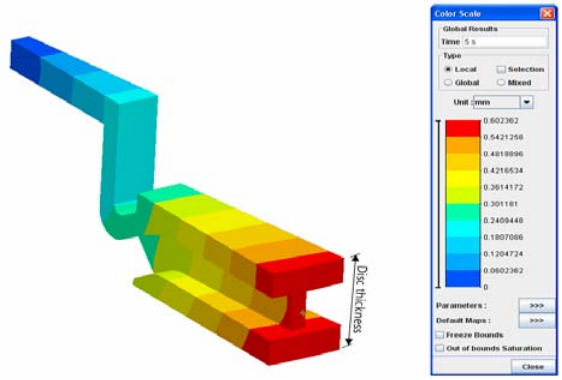

(a) Nodal displacement distribution of a disc

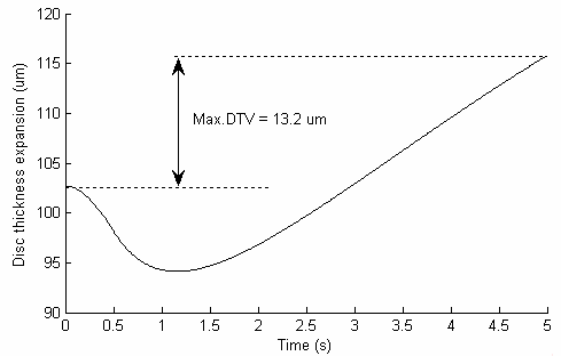

(b) Variation of the disc thickness

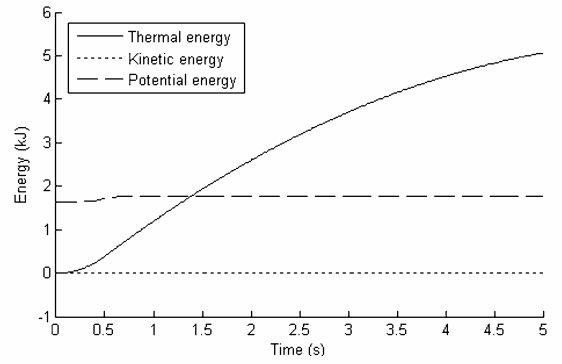

(c) Energy balance results

Fig. 9. Thermal analysis results.

5. Conclusions

The braking pressure transfer process of the hydraulic brake system was analytically derived. Based on information of the vehicle, brake and hydraulic devices, the heat flux for the front disc was calculated. From braking performance graphs such as the booster in/out force and braking pressure, we know that the braking characteristics of the system are exactly described according to the initial design settings. The thermo-mechanical analysis was performed by applying heat flux to the finite element model of a piece of disc, and the temperature rise and DTV were obtained. The simulation results show

that the variations of disc temperature and thickness are also affected by the characteristics of the brake system. Therefore, the thermal performance of a disc, which is changed by the vehicle and brake system characteristics, can be predicted using the proposed analysis process, and this prediction is very important in the design stages of a vehicle. In the future, the optimum shape of a disc will be investigated, and the thermal performances of the initial and optimum discs will be compared.

References

[1] F. Talati and S. Jalalifar, Analysis of heat conduction in a disc brake system, *Heat Mass Transfer*, 45 (2009) 1047-1059.

[2] J. T. Kim and B. J. Baek, A numerical study of thermal performace in ventilated disk brake, *Journal of the Korean Society of Tribologists & Lubrication Engineers*, 17 (5) (2001) 358-364.

[3] Y. Choi, J. W. Choi, H. M. Kim and Y. W. Seo, Thermal dissipation performance of the ventilated brake disc having helical grooved vent, *Journal of the Korean Society of Precision Engineering*, 21 (3) (2004) 117-123.

[4] S. M. Kim, A study on thermal analysis in ventilated brake by FEM, *Journal of the Korean Society of Machine Tool Engineers*, 18 (5) (2009) 544-549.

[5] P. Hwang, H. C. Seo and W. Xuan, A study on temperature field and contact pressure in ventilated disc-pad brake by 3D thermo-mechanical coupling model, *Journal of the Korean Society of Tribologists & Lubrication Engineers*, 25 (6) 421-426.

[6] S. P. Jung, K. J. Jun, T. W. Park and J. H. Yoon, Development of the brake system design program for a vehicle, *International Journal of Automotive Technology*, 9 (1) (2008) 45-51.

[7] K. J. Jun, T. W. Park, S. P. Jung, S. H. Lee and J. W. Yoon, Development of a numerical method to predict the alpine test result, *Proceedings of the Institute of Mechanical Engineers, Part. D*, 222 (2008) 1841-1849.

[8] Samcef User's Manual, Ver.13.1, 2010.

Won Sun Chung works for Korea Automotive Technonoly Institute as a senior resercher. He is now focusing on the judder vibration of a passenger vehicle, and the hot judder phenomenon of the disc brake is one of his major interests. Also, he studies computational engineering and optimization.

Tae Won Park received a B.S. in Mechanical Engineering from Seoul National University. He then went on to receive his M.S. and Ph.D. degrees from the University of Iowa. Dr. Park is currently a Professor at the School of Mechanical Engineering at Ajou University in Suwon, Korea.